Polymer–Leather Composites. IV. Mechanical Properties of Selected Acrylic Polymer–Leather Composites

EDMUND F. JORDAN, JR., BOHDAN ARTYMYSHYN, and STEPHEN H. FEAIRHELLER, *Eastern Regional Research Center,* Philadelphia, Pennsylvania, 19118*

Synopsis

An extensive study was made of the mechanical properties of the polymer–leather composite materials reported in previous articles. Polymer was deposited into leather by both emulsion and bulk (or solution) polymerization. Either methyl methacrylate, *n*-butyl acrylate, or a fixed comonomer mixture of *n*-butyl acrylate and methyl methacrylate were used over the widest feasible range of composition. Tensile strengths, in analogy with many polymer-treated fibers, were generally smaller than untreated controls, but entensions to break remained fairly constant as composition changed. Polymer–leather composites prepared by both methods were rheologically similar when correlated against the volume fraction of the polymer used. Relative tensile and torsional moduli were greater than unity at small volume fractions of polymer, but higher compositions assumed more of the viscoelastic characteristics of the modifying polymer. The constancy of the glass transition temperature of the polymeric component as composition changed indicated poor domain interactions. However, residual porosity reduced low-temperature moduli anomalously. A modified Halpin–Tsai equation was proposed that qualitatively predicted moduli increase by incremental space filling as either fiber aggregation (from simple air drying of untreated controls) or polymer content increased. The simultaneous rheological dependence of polymer–fiber interactions in composites was also accounted for by the equation.

INTRODUCTION

This article presents a comprehensive study of the mechanical properties of composite materials composed of selected acrylate polymers deposited in chrome-tanned cattlehide by free-radical polymerization.† It is the fourth in a series wherein the general characteristics,[1] kinetics,[2] and composite morphology[3] of these materials have been reported. The entire series is concerned with the use of a convenient process[4–6] for depositing selected acrylate polymers in leather by polymerization in the fibrous matrix. Two depositing procedures were followed: (1) polymer was introduced, *in situ,* into hydrated leather panels by emulsion polymerization initiated by a potassium persulfate–sodium bisulfite redox system, and (2) the free space in dry panels was incrementally filled by means of a bulk or solution polymerization technique. Composites were prepared from methyl methacrylate, a comonomer mixture of methyl methacrylate and *n*-butyl acrylate (containing 59.1% of the latter), and *n*-butyl acrylate, thus

* Agricultural Research, Science and Education Administration, United States Department of Agriculture.

† Reference to brand or firm name does not constitute endorsement by the U.S. Department of Agriculture over others of a similar nature not mentioned.

Journal of Applied Polymer Science, Vol. 26, 463–487 (1981) CCC 0021-9885/81/0026-0463$02.50

introducing a wide spread in glass transition temperature (T_g) contributed by the modifying polymer.

The previous work revealed that a controlling grafting mechanism, involving primary radical attack to collagen,[7a,8,9] was precluded.[1,2] Instead, polymer was shown to deposit, from coalescing emulsion particles, preferentially in layers near panel surfaces to form coarse strongly adsorbed deposits around individual fibers in fiber bundles that resisted benzene extraction. In the present work, mechanical properties were determined on selections from the large number of experiments collected in the former studies.

Previous discussions of the mechanical properties of cotton and wool and other natural fibers and fabrics containing grafted and deposited polymer, and included as part of reviews,[7b,11,12] are pertinent to this work. In general, for treated cotton fibers, tenacity,[13–16] break toughness,[13–15] and stiffness[13–15] generally, but not always,[17] decreased while elongation remained essentially constant with increase in polymer content for high-modulus polymers at ambient temperature and humidity. Similarly, treated cotton fabrics, while generally retaining these properties, demonstrated additional good flex and flat abrasion resistance.[15,18,19] Wool fibers[7,20–23] and fabrics[24] exhibited somewhat similar properties in spite of differences in the tensile dynamics of untreated wool,[7b,25,26] but these again depended on the viscoelastic properties of the modifying polymer.

Leather possesses some of the characteristics of a natural fabric, although it is much thicker and has a three-dimensional random weave.[3] Diameters of the individual fiber bundles vary (15–200 μm) and consist of densely deposited fine fiber bundles in an upper or grain layer; these bundles become abruptly coarser and randomly interlocked in the lower corium or strength-bearing region of cattlehide leather. However, size aggregation in the microfine region bears some resemblance to cotton and wool.[1,3]

The mechanical properties of untreated leather have been reviewed[27] together with aspects of viscoelasticity.[28] Special studies on effect of location[29–32] and splitting,[33] together with creep,[34] hysteresis,[35] and dynamic mechanical properties of collagen films[36] and leather[37] are available. The mechanical properties of fibers teased from leather have also been reported.[27,38,39] While the effects of polymer impregnants on mechanical properties have been studied,[40–42] the available articles on graft polymerization have produced only a few studies on tensile strength and specific leather tests,[43–45] including stiffness of grafted sheepskins.[6]

In this article tensile strengths, elongations, tensile dynamics, tensile moduli, and torsional moduli, the latter at 23°C and as a function of temperature, are assembled on selections of the composites prepared in parts I, II, and III. Some of the emulsion-prepared composites were isolated by methanol extraction (or acetone and methanol extraction, controls) to remove water and preserve the expanded matrix by minimizing apparent density. Others were then benzene extracted to isolate the effect of the bound polymer alone. Selections were simply air dried to stiffen the untreated controls by increasing their density. The effect of polymer in preventing fiber aggregation could then be obtained. Finally, the effect of volume fraction of modifying polymer on modulus ratios (between composites and their controls) were treated qualitatively with current theories for particulate and fiber filled composites.[46a,46b]

EXPERIMENTAL

Starting Materials

As discussed in detail in part I[1] of this series,[2,3] the chrome-tanned cattlehide panels used to make the composites for this article were approximately 0.23 cm thick (5 oz) before polymer treatment and after acetone drying. The polymer was introduced by emulsion polymerization in water-soaked panels, or by bulk or benzene solution polymerization with bis-azoisobutyronitrile as initiator into acetone dried panels, also as described in part I. The air-dried panels (controls and polymer treated) were given no solvent treatment (acetone, methanol, or benzene), but were dried in a forced air draft and then conditioned at 50% RH prior to being tested. Because removal of water by solvent prevents stiffness, the air drying increased stiffness.

Mechanical Properties

Tensile strengths, percent elongations, and tensile moduli were obtained on an Instron tensile tester, model TTB, following leather-testing procedure ASTM D2209-64 (reapproved 1970) at 23°C and 50% RH. Test specimens were taken perpendicular to the backbone from panels cut at all consecutive locations starting at the rump.[27,29–31] The effect of natural variability was minimized by pairing each treated panel with an adjacent untreated control. Initial tensile moduli were taken from stress–strain curves with

$$E = (F/A)/(\Delta L/L_0) \tag{1}$$

where F is force in pounds, A is cross-sectional area in inches,^{2} and $\Delta L = L - L_0$, where L is the length corresponding to the force F, and where L_0 is the initial specimen length, both in inches. The modulus of the next linear portion of the curve (see below) was obtained by a modification of eq. (1) as

$$E_f = (F/A)/[(L - l_0)/(L_0 + l_0)] \tag{2}$$

where L is the length to break and l_0 is the extension increase after the initial displacement in eq. (1) by extrapolation to the absissa.

Torsional modulus data were obtained by the method of Williamson[47]; the procedures used followed ASTM Standards D1043-61T, with the Clash–Berg method.[48] The relation between these methods has been discussed.[49]

Definitions

The notations of parts I, II, and III were followed here. All references to the starting polymers and the composite systems are by abbreviations for their monomers, as follows: methyl methacrylate, MMA; fixed composition copolymer, n-butyl acrylate–methyl methacrylate, BA + MMA; and n-butyl acrylate, BA. Weight fraction is w_i, but volume fraction, ϕ_i follows the customary notation used for composite materials.[46a,46b] Subscript 2 always refers to polymer and subscript 1 to the leather matrix; E and E_t to Young's tensile and torsional moduli, respectively. Rupture energies in lb in. were taken from electronic integration of stress–strain curves, with the data converted to ergs cm^{-3}. All curve fitting was done with an IBM 1130 computer.

RESULTS AND DISCUSSION

General Features

Table I lists tensile strengths, elongations, rupture energies, and tensile and torsional moduli at 23°C for about half of the emulsion-prepared methanol extracted composites (sections A, B, C) with a few selections of the corresponding bulk or solution prepared composites for the BA + MMA system only (section D). Data on MMA and BA bulk-solution prepared composites and on benzene-extracted composites and other experiments missing from all of the sections resembled the data in the table at similar compositions. Missing data are included in more detailed treatments below. Table I lists only the average values of the mechanical properties for all controls (experiment 1).

As will be seen, variability was large for individual control values; therefore, relative trends are not always readily ascertainable by use of this average value. Consequently, the experimental relative values between the composite and its control TS/TS_1 (and the corresponding modulus ratios) reflect actual behavior more accurately. All systems showed either no change or slight decreases in tensile strength compared to their controls for the majority of composites tested. Extensions to break remained fairly constant compared to controls except at high w_2 for MMA and BA + MMA composites, where they decreased. They were uniformly higher than controls for BA systems.[4,6,43–45] This is typical behavior for polymer-grafted natural fibers and fabrics.[7b,11–24] The restrictive morphology characteristic of these systems[3] is clearly reflected in their tensile and torsional moduli and, more importantly, in their relative values, E/E_1 and E_t/E_{t1}, respectively. All three systems generally showed increased stiffness compared to controls, $(E_i/E_{i0} > 1)$, whether made in emulsion or bulk solution. However, the order in $d(E_i/E_{i0})/dw_2$ was MMA > BA + MMA > BA. At higher w_2, stiffness ratios decreased slightly from their maximums as w_2 approached unity for BA + MMA and BA. This aspect of the work is discussed in detail in the following sections.

Considerable internal inconsistancy and variability can be seen in the limited data presented on properties with changes in w_2 in Table I. These trends were more apparent when all of the available data were examined. This is attributed, in large part, to natural variability of the untreated leathers, although the complex processes affecting individual deposition probably played a role.[1,2] As will be seen, however, statistical correlation of the data revealed mathematically significant trends that are internally consistant and are generally in harmony with current knowledge of composite materials, even though individual experimental variation was sometimes considerable.

Tensile Strength and Tensile Moduli

Typical stress–strain curves are presented in Figure 1. (A) is the curve for the average of the untreated controls. It is typical of split cattlehide. The initial relatively low modulus, Young's modulus E [experiment (1), Table I], probably reflects a preponderance of fiber conformational displacements, resisted largely by frictional interaction accompanied by some drawn collagen fiber contributions[27,28,36,46b] as fibers became taut in straining.[34] The second or upper modulus region, E_f [eq. (2)], is thought to involve mostly bulk straining, with its magnitude

reduced to the extent that fibers break or become untangled and slip. Figure 1, insert B, presents typical curves for composites of polymer composition, increasing from curves 1 to 4, for the MMA and BA + MMA systems. At some critical concentration that increased as T_g for the base polymer decreased, the curve shape changed from that of the controls [Fig. 1(A)] and E became discontinuously large (curves 2 and 3) while E_f decreased. This effect lead eventually (curve 4) to brittle failure.[46c,46d] Specific experimental data for load-extension curves are shown in Figure 2. Insert A illustrates the type of variability found for the control samples whose tensile value is presented as experiment 1 in Table I. Although these data involved an average for all locations in the hide so that variability was maximized,[29–32] the use of matched panels for controls and treated samples only partially alleviated the uncertainty produced by the natural variability. Beyond critical values of w_2 and ϕ_2, all MMA and BA + MMA composites [Figs. 2(B) and 2(C)] showed the discontinuous increase in initial modulus alluded to in Figure 1 (curves 2 and 3). Although the BA systems [Fig. 2(D)] did not show this effect, their moduli were generally greater than the average of the controls (dashed line). This appears to reflect the restriction imposed on the fibers resulting from their being encased in polymer, which was demonstrated to be the major morphology for these systems in part III.[3] Consequently, the initial modulus increased appreciably with increasing polymer content. In addition, the reduction in volume fraction of free space,[1] as polymer content increased, further reduced the free movement of all fiber aggregates[3] when the composites were strained. This is seen better from a correlation of the tensile modulus ratios E/E_1 as a function of the volume fraction of polymer, ϕ_2. Before proceeding, ϕ_2 requires definition.

The volume fraction of polymer in 1 g of emulsion-prepared polymer–leather composite, regardless of isolation method, is given by[1]

$$\phi_2 = W_2/\rho_p/(W_2/\rho_p + W_1/\rho_{a0}) \tag{3}$$

Consequently, the volume fraction of leather is $1 - \phi_2 = \phi_1$, where $W_i = (W_1 + W_2)\, w_i$ with w_i the weight fraction of the components. The quantities ρ_p and ρ_{a0} are the apparent densities of polymer and leather, respectively. It was observed in part I that density was, in principle, a simple linear function of ϕ_2 and followed, for 1 g of the composite $W_1 + W_2$,

$$\rho_a = 1/[W_1/\rho_r + W_2/\rho_p + \phi_{f0}(W_1/\rho_{a0})] = \phi_1\, \rho_{a0} + \phi_2\, \rho_p \tag{4}$$

where ρ_r is the real density of leather, obtained by use of a helium air pycnometer,[1] and ϕ_{f0} is the volume fraction of free space in the initial leather, having a density ρ_{a0}. However, a vertical shift between experimental data and the theoretical curve of eq. (4) required introduction of a small factor (ρ_{a0}/ρ_i) to account for initial filling of small pores. With this correction, for 1 g of composite,

$$\rho_a = 1/\{W_1/\rho_r + W_2/\rho_p + [\phi_{f0}(W_1/\rho_{a0})\rho_{a0}/\rho_i]\} \tag{5}$$

Consequently, the volume fraction of polymer ϕ_2 becomes

$$\phi_2 = W_2/\rho_p/\{W_2/\rho_p + W_1/\rho_r + [\phi_{f0}(W_1/\rho_{a0})]\rho_{a0}/\rho_i\} \tag{6}$$

As discussed previously,[1] average values for untreated leather densities for emulsion systems and bulk-solution systems were slightly different; both are listed with other leather constants in Table II.

TABLE I
Tensile Strengths, Elongations, Rupture Energies, Tensile and Torsional Moduli, and Composite–Leather Moduli Ratios for Selected Data[a]

Experiment No.	Composition		Tensile properties at 23°C					Torsional moduli at 23°C		
	w_2	ϕ_2	TS, psi	Extension to break, %	E^b, psi	$E/E_1{}^c$	$TS/TS_1{}^c$	E_t, psi	$E_{t1}{}^c$, psi	E_t/E_{t1}
			(A) Poly(methyl Methacrylate)–Leather Composites, Methanol Extracted							
1	0[d]	0	1,722	61.3	1,290	1	1	1,944	1,944	1
2	0.103	0.0543	1,725	44.3	5,550	4.18	1.03	1,300	980	1.33
3	0.258	0.145	1,560	42.8	8,980	5.51	0.650	7,800	1,500	5.20
4	0.470	0.288	1,395	31.5	41,400	20.5	0.542	29,000	1,430	20.3
5	0.657	0.439	918	3.5	39,400	25.2	0.461	37,000	1,200	30.8
6	1.0	1.0	7,760[e]	5.0[e]	220,000[e]	165.7	4.51	540,000	1,944	27.8
			(B) Poly(*n*-Butyl Acrylate-*co*-Methyl Methacrylate)–Leather Composites, Methanol Extracted							
7	0.0875	0.0478	2,105	55.5	3,335	1.48	0.907	2,800	2,300	1.22
8	0.184	0.105	1,305	51.8	5,430	1.67	0.653	4,600	1,600	2.88
9	0.304	0.182	1,230	31.0	12,800	3.68	0.898	12,000	970	12.4
10	0.523	0.344	1,950	30.0	16,000	12.8	0.692	15,500	2,400	6.46
11	0.601	0.411	1,440	24.8	12,500	8.03	0.850	14,000	1,620	8.64
12	1.0	1.0	2,113[e]	275[e]	17,940[e]	8.85	1.123	2,300	1,944	1.183

(C) Poly(*n*-Butyl Acrylate)–Leather Composites, Methanol Extracted										
13	0.113	0.0642	1,485	109	1,050	0.779	1.18	3,300	3,800	0.868
14	0.233	0.139	2,530	82.0	3,110	1.54	0.821	4,800	4,300	1.12
15	0.578	0.406	1,580	48.3	2,140	1.51	0.854	2,500	2,000	1.250
16	1.0	1.0	(10)[e]	>1000[e]	13.1[e]	0.0071	0.0042	61	1,944	0.0314
(D) Poly(*n*-Butyl Acrylate-*co*-Methyl Methacrylate)–Leather Composites, Bulk Solution										
17	0.174	0.120	2,260	82.5	2,778	1.83	1.16	6,500	1,860	3.50
18	0.254	0.192	2,160	45.0	17,500	8.52	1.02	30,000	3,220	9.32
19	0.543	0.528	2,505	38.8	18,800	30.1	1.44	42,000	1,670	25.15

[a] Partial list of the available data selected to illustrate trends. Data on the balance (~71 experiments plus controls) are included as components in the various graphs and tables below.

[b] Modulus E is initial modulus. Average values of E_f, the final modulus of the stress–strain curves, are, for the emulsion systems, in psi: controls, 6220; MMA, 6292; BA + MMA, 3866; BA, 3803. For bulk solution, 3440 psi.

[c] E_1 is the tensile modulus and E_{t1} the torsional modulus of each untreated experimental control leather. TS_1, is the tensile strength of an untreated control leather paired with each sample.

[d] Average values of the control tensile data taken by reference to Fig 2(A).

[e] From ref.[61].

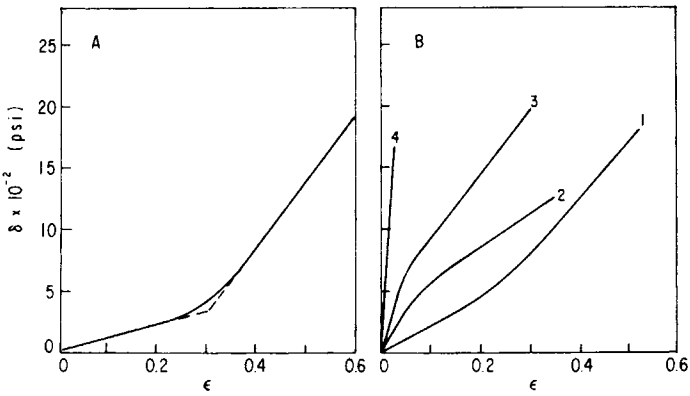

Fig. 1. Typical stress–strain curves showing characteristic linear regions. (A) Averaged curve for all untreated controls. (B) Typical composites selected as follows: curve 1, MMA, $w_2 = 0.182$; curve 2, BA + MMA, $w_2 = 0.280$; curve 3, BA + MMA, $w_2 = 0.523$; curve 4, MMA, $w_2 = 0.504$.

For composites made by the bulk or solution technique (Table I), where polymer was formed exclusively in the unswollen leather matrix, depletion of free space occurs rapidly with w_2 increase. Consequently,

$$\phi_2 = W_2/\rho_p/(W_2/\rho_p + W_1/\rho_{a0}') \tag{7}$$

where ρ_{a0}' is the density of 1 g leather with its free space partially occupied by depositing polymers[1];

$$\rho_{a0}' = 1/\{1/\rho_r + [\phi_{f0}\,(1/\rho_{a0}) - (W_2/\rho_p)\rho_r/\rho_p]\} \tag{8}$$

Thus, eqs. (6) and (7) yield a common parameter ϕ_2 that enables both preparation methods to be compared without the conceptual difficulty imposed by different residual free-space volumes inherent in the use of w_2.

To correlate experimental modulus ratios directly, the equation

$$\ln(E/E_1) = [\ln\,(E/E_1)]_0 + \alpha\phi_2 - \beta\phi_2^2 + \gamma\phi_2^3 \tag{9}$$

was found by computer estimate to fit all of the data significantly, even though γ was often zero. Because $[\ln(E/E_1)]_0$ was close to zero, all data were forced through the origin.

Tensile modulus ratios are plotted against ϕ_2 in Figure 3. (A) (MMA) illustrates the considerable scatter, especially severe because the logs of the modulus ratios are used. Of special significance is the common correlation with ϕ_2 of all tensile modulus data, regardless of the method of preparation. Figs 3(B)–3(D) which present data [fitted by eq. (9), solid line] for MMA, BA + MMA, and BA, respectively, against ϕ_2, were all insensitive to the method of composite preparation. Thus, it was simply the depletion of free space, V_a, in the matrix and the interaction of polymer and collagen fibers that controlled the composite modulus. Insight into this interaction can be obtained through the use of equations originally derived to predict the mechanical properties of particulate-filled polymers.

A general form of several specific equations useful for correlating modulus ratios with composition for composite materials, such as those of Mooney,[50] Kerner,[51] and the equivalent equation of Haskin–Shtrikman,[52] is that attributed to Tsai[53] and Halpin,[54] as modified by Nielsen[46a,46b]:

$$E/E_1 = (1 + A\,B\,\phi_2)/(1 - B\,\psi\,\phi_2) \tag{10}$$

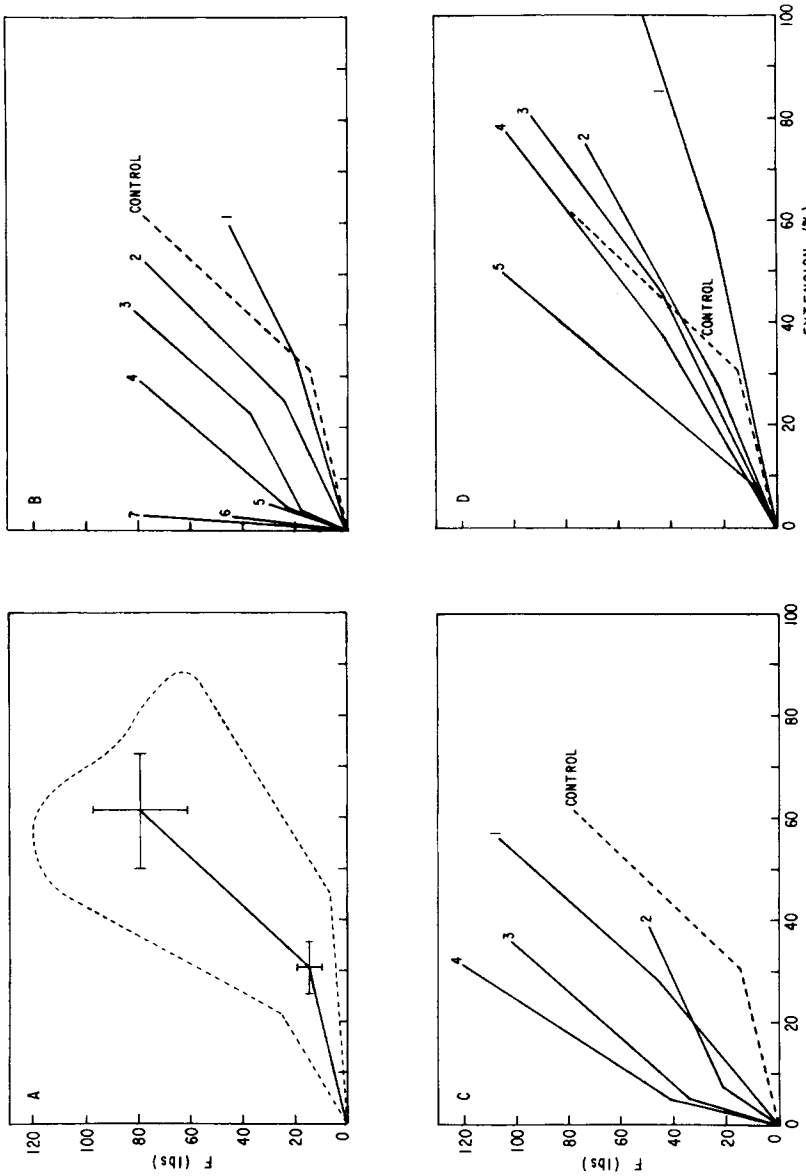

Fig. 2. Simplified force-extension curves. (A) Averaged curve for all untreated controls. Bars designate standard deviations of both force and extension for each linear region and dotted envelope approximately extreme limits observed. (B)–(D) Typical curves for emulsion-prepared composites. Curve numbers designate polymer compositions, w_2, as follows: curve, w_2; (B) (MMA): (1) 0.081; (2) 0.182; (3) 0.258; (4) 0.351; (5), 0.235; (6), 0.518; (7) 0.657. (C) (BA + MMA): (1) 0.088; (2) 0.280; (3) 0.389; (4) 0.523. (D) (BA): (1) 0.133; (2) 0.156; (3) 0.208; (4) 0.303; (5) 0.578.

TABLE II
Comparison of Leather Constants

Constants Used in this Article

Parameters	Untreated leather controls: Emulsion	Untreated leather controls: Solution	Modifying polymer densities, g cm^{-3}: MMA	BA + MMA	BA
ρ_{a0} g cm^{-3}	0.5556 ± 0.027	0.6241 ± 0.037	1.146	1.103	1.072
ϕ_{f0}	0.6125	0.5648	T_i = 110°C	T_i = 13°C	T_i = −49°C
ρ_{a0}/ρ_i	0.9238		T_g = 105°C	T_g = 8°C	T_g = −54°C
ρ_r g cm^{-3}	1.434				

Halpin–Tsai Equation [eq. (10)] Constants

System	Temp., °C	Tension: A	Tension: B	Tension: E_2, psi	Tension: E_1, psi[a]	Torsion: A	Torsion: B	Torsion: E_2 psi	Torsion: E_1, psi
MMA	23	70.44	0.697	220,000	1,328	42.53	0.864	540,000	1,944
BA + MMA	23	17.90	1.0	∞	2,028	27.63	1.0	∞	1,944
BA	23	0.884	1.0	∞	1,841	0.324	1.0	∞	1,944
All data	T_i − 50					69.69	0.7218	315,000	1,708
All data	T_i + 50					2.95	1.0	∞	1,203
Air-dry controls	23	103.5	0.862	870,200	1,328	268.2	0.625	870,200	1,944

Modified Halpin-Tsai Equation [eq. (17)] Constants

System	Tension: E_p, psi	Tension: E_c, psi	Tension: $\ln(E_p/E_c)$	Torsion: E_p, psi	Torsion: E_c, psi	Torsion: $\ln(E_p/E_c)$
MMA	220,000	870,200	−1.358	335,000	870,200	−0.9546
BA + MMA	17,940	870,200	−3.882	2,300	870,200	−5.936
BA	13.1	870,200	−11.104	61	870,200	−9.566

[a] Average of control moduli for each system.
[b] Computed by use of eq. (16).

where E is any modulus, (shear, Young's, or bulk) and E_1 is the modulus of the matrix. For reinforced rubbers, E_1 is the softer component. The constant A accounts for the geometry of the filler phase and Poisson's ratio of the matrix. Thus, A is related to the Einstein coefficient k_E of the viscosity equation

$$\eta = \eta_1 (1 + k_E \phi_2) \tag{11}$$

which increases as the filler geometry passes from spheres (k_E = 2.5) through elongated ellipsoids to rodlike agglomerates. For example, when aspect ratios were 16, $k_E > 10$.[46a] Thus, A is defined in terms of k_E as

$$A = k_E - 1.0 \tag{12}$$

As the magnitude of A increases toward $A = \infty$, increased parallel packing is implied[46a,55]; as A approaches zero, series packing is dominant. Thus, A is a fairly sensitive indicator of the type of packing involved in the composite. The quantity B, on the other hand, accounts for the relative modulus of the filler and matrix phases; its value is nearly 1.0 for large E_2/E_1 ratios

$$B = [(E_2/E_1) - 1]/[(E_2/E_1) + A] \tag{13}$$

The quantity ψ in eq. (10) is related to the maximum packing fraction ϕ_m of the filler[46a] above, in which phase inversion commences, through

$$\psi = 1 + [(1 - \phi_m)/\phi_m{}^2]\phi_2 \tag{14}$$

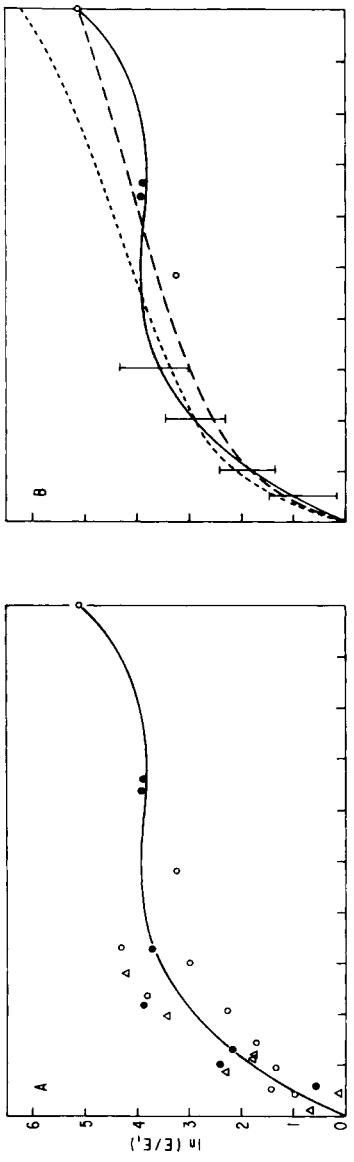

Fig. 3. Log of modulus ratio in tension $\ln(E/E_1)$ for composites relative to their controls, (E_1), vs. volume fraction of polymer in composite, ϕ_2. (A) Computer-fitted curve [eq. (9)] drawn through all MMA data. ○, Methanol extracted; △, benzene extracted; ●, bulk-solution prepared. (B) (MMA), (C) (BA + MMA), and (D) (BA) curves were fitted by computer, eq. (9), (solid lines) and by constants (Table II) of Halpin–Tsai equation, eq. (10) (wide dashed lines) and modified Halpin–Tsai equation, eq. (17), (short dashed line). Bars represent extremes of experimental scatter indicated by actual experimental points similar to (A) for all methods of preparation and treatment.

and

$$\psi \phi_2^2 = 1 - e^{-\phi_2/[1-(\phi_2/\phi_m)]} \quad (15)$$

because $\psi\phi_2$ is a reduced volume fraction. Consequently, as $\phi_m \rightarrow 1$, $\psi \rightarrow 1$, and phase inversion becomes forbidden.

In the broadest sense, untreated leather can be considered to be a composite of fibers which are free to move with frictional constraints in restricted free space within limits imposed by attachment to a continuous matrix. Under strain, this free space is reduced and the modulus rises [Figs. 1(A) and 2(A)] as frictional restraints and orientation effects retard further straining. Polymer or any type of penetrating liquid also reduces free space so that the modulus should be initially increased if that liquid is viscous enough. As seen in Figures 3(B)–3(D), interaction between polymer and bulk fiber becomes increasingly important as ϕ_2 approaches unity and as V_a approaches zero [eq. (6) or eq. (7)], thus altering curve shape for different systems.

Correlation of the data (Table I) with the Halpin–Tsai equation (Fig. 3, wide dashed lines) was accomplished by arbitrarily designating the untreated leather to be the soft component with modulus E_1, and the polymer to be the particulate filler, of modulus E_2. This clearly violates assumptions concerning isotropic purity of the phases[52] and discreteness of the domain sizes.[56a] It is justified merely as a convenient empirical relation having some theoretical significance under special circumstances, and because macrodimensional domain sizes do not seem to alter relative moduli appreciably.[55]

The quantity A was estimated for all three systems [eq. (10)], curve fitted in Figure 3, from moduli ratios taken at ϕ_2 of 0.2 by use of eq. (9), with the reasonable assumption that ϕ_m and, therefore ψ, is unity. Values of B [eq. (13)] and A are listed in Table II. For MMA the fit of the curve (wide dashed line) in insert B is reasonable over all ϕ_2 and the magnitude of A implies mostly parallel packing. This appears to be logical[62a] for a morphology where, with increasing ϕ_2, free space is reduced[1] (abruptly decreasing the influence of the initial leather matrix) and where fibers, aligned more or less parallel, are restricted by encasement in a hard polymer. Thus, rapid and continuous increase in modulus with w_2 increase is expected. Because of the unrealistic assignment of B required to fit relative data at $\phi_2 = 0.2$ for BA + MMA in Fig 3(C) and BA in Fig. 3(D), values of A in Table II for these systems are merely empirical. The correlation is useful, however, because stiffness behavior over the practical preparative range of ϕ_2[1,2,4–6] can be predicted from only one or two experimentally determined values of E/E_1.

Relative tensile strengths (Table I) versus ϕ_2 are plotted freehand in Figures 4(A)–4(C) for all three composite systems. Noteworthy are the differences found between emulsion-prepared systems (solid and dashed lines) and bulk-solution systems (short dashed lines) especially for BA + MMA, [Fig. 4(B)] Analogous behavior was found for a few rupture energies, E_R, for the MMA composites, drawn freehand in Figure 4(D) and Figure 5. The reduction in E_R with ϕ_2 increase for MMA composites continued until brittle failure dominated properties at high ϕ_2 (Figs. 1 and 2), as is characteristic of MMA homopolymer.[46c] While all BA systems were relatively weak compared to leather [Fig. 4(C)] all were apparently toughened (Figs. 5(C) and 5(D)]. This was implied by their increased elongations[4,6,43–45] in Table I. However, because their tensile strengths were

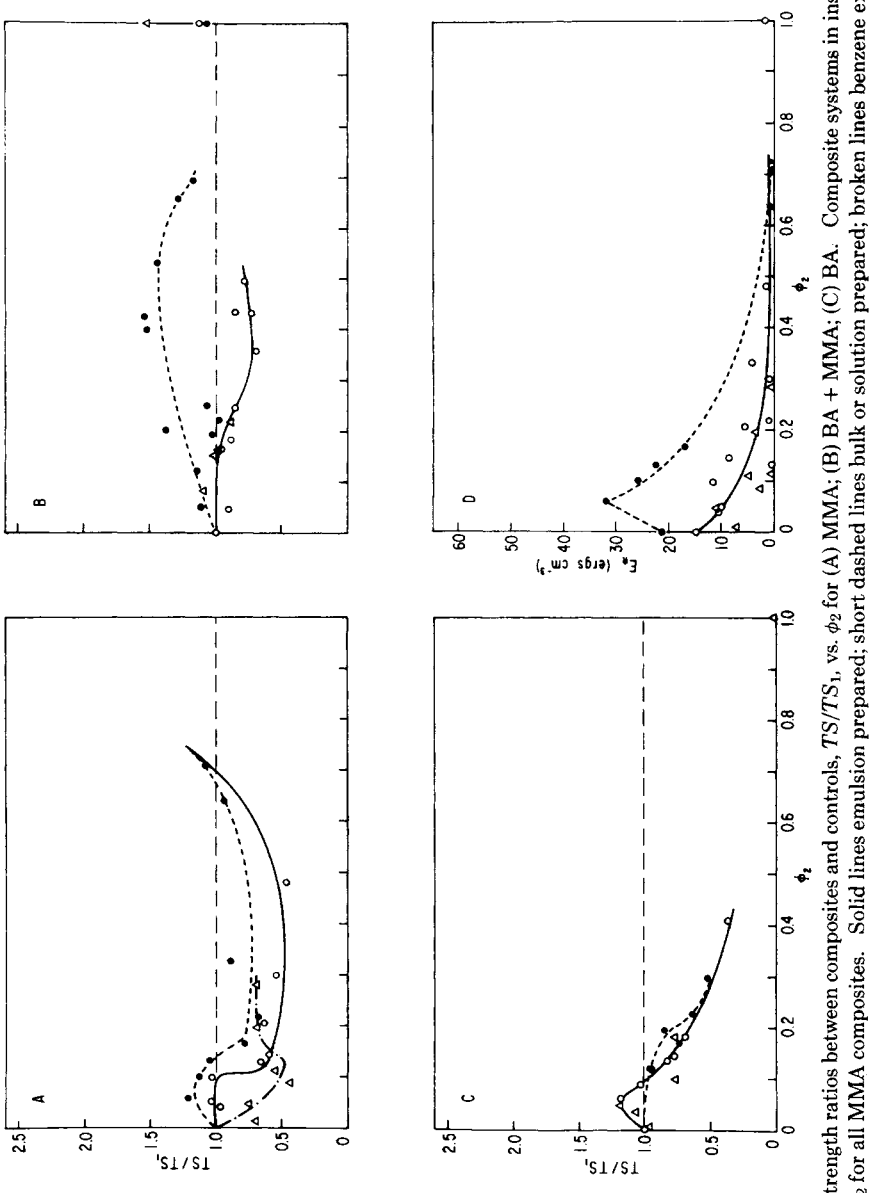

Fig. 4. Tensile strength ratios between composites and controls, TS/TS_1, vs. ϕ_2 for (A) MMA; (B) BA + MMA; (C) BA. Composite systems in insert D show rupture energies, E_R, vs. ϕ_2 for all MMA composites. Solid lines emulsion prepared; short dashed lines bulk or solution prepared; broken lines benzene extracted data.

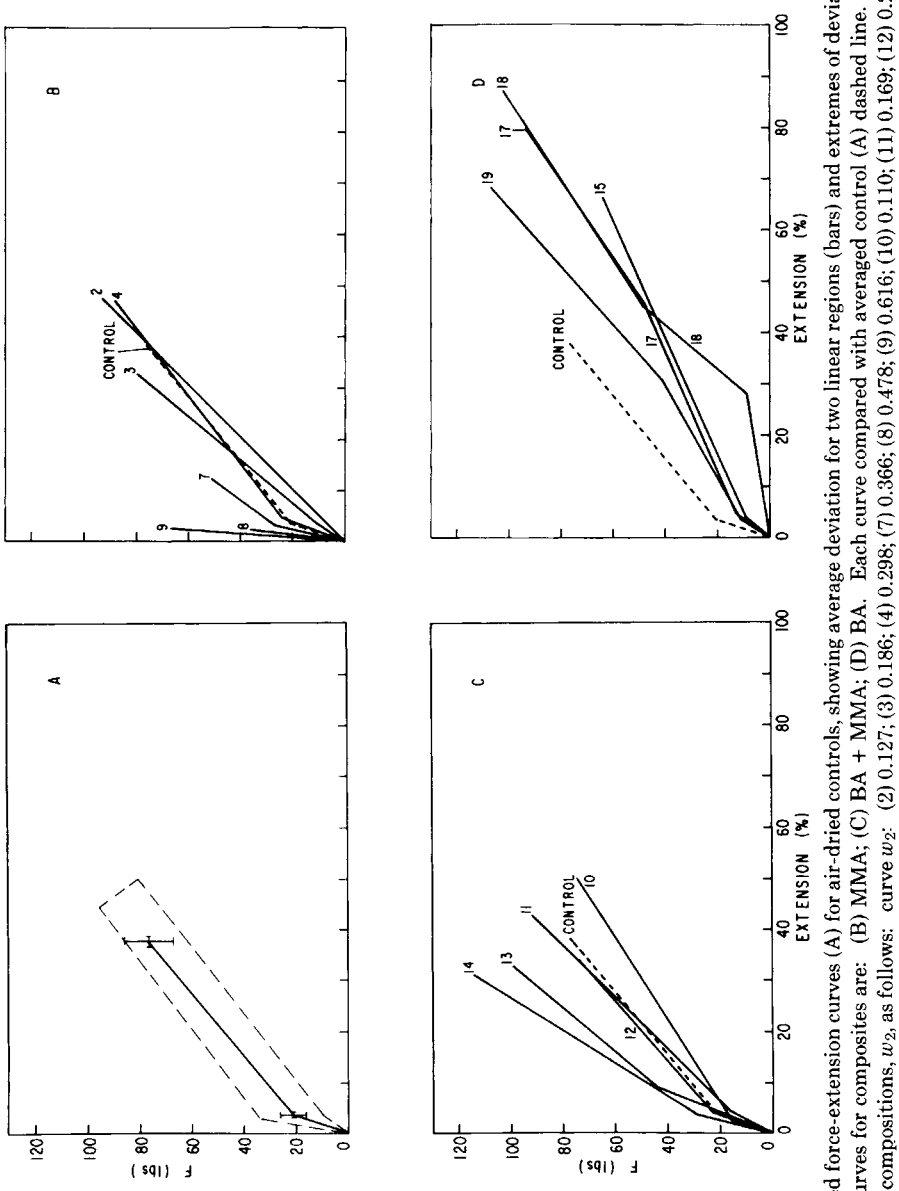

Fig. 5. Simplified force-extension curves (A) for air-dried controls, showing average deviation for two linear regions (bars) and extremes of deviation (short dashed lines). Selected curves for composites are: (B) MMA; (C) BA + MMA; (D) BA. Each curve compared with averaged control (A) dashed line. Numbered curves designate polymer compositions, w_2, as follows: curve w_2: (2) 0.127; (3) 0.186; (4) 0.298; (7) 0.366; (8) 0.478; (9) 0.616; (10) 0.110; (11) 0.169; (12) 0.276; (13) 0.277; (14) 0.372; (15) 0.079; (17) 0.199; (18) 0.278; (19) 0.314.

relatively small, much of the extra energy input was apparently consumed in flow.

The preferential packing of emulsion-prepared polymer in layers in cattlehide, constituting 20–60% of the cross section (discussed in detail in parts I and III and mentioned in the Introduction), appeared to have little effect on the mechanical properties, especially stiffness, when compared with mostly homogeneous composites (bulk solution)[3] for compositions of the same polymer volume fraction, ϕ_2. Either the deformation energy distributed itself quickly throughout the fibrous network in the emulsion systems, thus negating a skin effect,[46a] or its effect was obscured by compensating inconsistencies in the bulk-solution composites or by error range. A choice between these possibilities, and others not mentioned, is not possible at the present time.

Air-Dried Composites and Controls

Mechanical data similar to those in Table I are presented for air-dried composites and their controls in Table III. While many of the data on the untreated controls, notably tensile strength and extension, are similar in both tables, tensile and torsional moduli at 23°C were 12 and 17 times larger after the controls are air dried. Average apparent densities were 0.6492 g cm^{-3} for air-dried samples compared to 0.5556 g cm^{-3} for those acetone dried. Air drying appeared to raise moduli greatly by a combination of free-space reduction and increased fiber surface interaction; the latter especially serves to increase the apparent coefficient of friction between adjacent fibers. Polymer of small w_2 has little effect (E/E_1, and $E_t/E_{t1} < 1$), but ultimately, at higher w_2, the polymer phase viscoelasticity, inherent in their respective vitreous transitions, assumed control of all systems. The dynamics of this may be seen in Figure 5. Force-extension curves for untreated leathers, insert A, now resemble those of polymer-treated leathers [Figs. 1, 2, and 5,(B) and 5(C)]. In fact, BA composites were all much softer than their controls [Fig. 5(D)], indicating the primacy of the polymer component here in affecting mechanical properties for these systems. From this discussion, the analogy between space reduction, fiber aggregation, and polymer retardation of fiber movement is obvious; this phenomena is treated further in the last section of this article.

Torsional Modulus–Temperature Curves

Torsional modulus–temperature curves for the two modifying homopolymers and one copolymer used in this work are compared in Figure 6 with an average computer-fitted curve for untreated leather controls (wide dashed line). The latter relation was

$$\ln E_t = \ln E_{t0} - \alpha T \tag{16}$$

From averages of slopes, α, and intercepts, $\ln E_{t0}$, obtained after computer fitting each experimental control curve, the constants for emulsion controls were $\ln E_{t0}$, 7.653 psi; α, 3.50×10^{-3}. These constants were used to draw the curves in Figure 6. However, the limits of vertical variability (bars) in this curve were again great. Inflection temperatures, T_i, assumed in this work to be $T_g + 5$°C,[57] were taken at 14,500 psi (10^9 dyne cm^{-2})[58] and are marked by slashes on the polymer and

TABLE III
Mechanical Properties of the Air-Dried Composites and their Controls

Experiment No.	Composite composition		Tensile properties at 23°C					Torsional modulus at 23°C		
	w_2	ϕ_2	TS/TS_1	Extension to break, %	E, psi	E_1, psi	E/E_1	E_t, psi	E_{t1}, psi	E_t/E_{t1}
(A) Poly(methyl Methacrylate)–Leather Composites Air Dried										
1	0	0	1.0[a]	38.1[b]	—	15,700[b]	1	—	32,000[b]	1
2	0.127	0.069	1.0	47.5	4,660	13,100	0.355	18,000	31,200	0.577
3	0.331	0.191	0.764	32.8	8,650	7,205	1.20	29,400	29,300	1.01
4	0.478	0.292	0.744	2.8	49,400	17,600	2.81	103,000	39,500	2.61
5	0.616	0.404	0.536	3.0	42,900	17,800	2.41	185,000	51,000	3.63
(B) Poly(n-Butyl Acrylate-*co*-Methyl Methacrylate)–Leather Composites, Air Dried										
6	0.110	0.061	1.03	51.5	5,510	18,600	0.296	8,400	14,100	0.596
7	0.169	0.97	1.01	42.5	10,100	22,000	0.459	13,800	24,000	0.575
8	0.372	0.206	0.938	30.5	16,900	22,100	0.765	22,000	37,000	0.595
(C) Poly(n-Butyl Acrylate)–Leather Composites, Air Dried										
9	0.079	0.044	1.04	64.5	7,040	12,700	0.554	13,300	28,000	0.475
10	0.199	0.117	1.33	90.0	6,200	8,550	0.725	6,600	30,000	0.220
11	0.314	0.194	0.891	68.0	5,410	13,700	0.395	6,500	25,000	0.260

[a] The average air-dried control tensile strength was 1,871 psi.
[b] Average values.

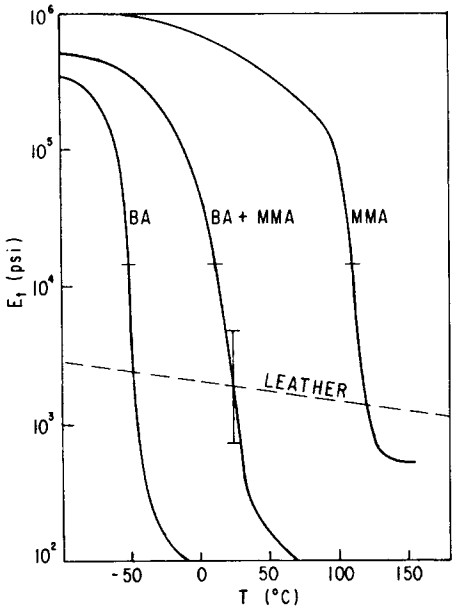

Fig. 6. Torsional moduli (E_{t2}) vs. temperature curves for base homo- and copolymers of this work (solid curves) and average curve (E_{t1}) for methanol- and benzene-extracted leather controls, calculated using eq. (16). Slashes indicate approximate inflection temperature, T_i, at 14,500 psi (10^9 dyne cm^{-2}) T_g estimated as T_i −5°C (Table II). Bar denotes extremes of variability of leather apparent moduli at 23°C.

copolymer curves. The large modulus span encompassed by the typical polymer curves contrasts dramatically with the featureless leather curve,[28,36,59] where transitions, other than those associated with water losses,[36] are not seen till a temperature of 175°C[28] is reached. The contrast is severly reduced (Fig. 7) when selections of emulsion-prepared and methanol-extracted composites are compared. The figure reveals stepped modulus–temperature curves[46e,56b,58] typical of composites possessing marked phase incompatibility. In confirmation of this, T_g values (downward arrows) were insensitive to changes in composition for each composite type. The upper deflection of the curve assemblies, produced by passage through the collagen T_g region (198°C),[28] were not reached in the experiments. However, these curves are anomalous in that at temperatures substantially below T_g (T_g − 50°C) equilibrium composite moduli were affected by composition. They did not reach a common plateau modulus of around 3×10^{10} dyne cm^{-2} (435,000 psi)[56b] typical of conventional composites. In contrast, compositional insensitivity was exhibited by these composites at temperature above their T_g. The composite plateaus, especially BA + MMA and BA, fall near that of leather regardless of composition. These anomalies suggest loose averaging of mechanical behavior from two independent systems rather than reflecting weighted contributions from mixed isotropic microdomains. The residual free space remaining as polymer content is increased[1,3] appears to be reasponsible for the apparent anomalies; each system is, in effect, a tricomponent composite of collagen, air, and polymer.

Differences between modulus–temperature curves for emulsion-prepared and bulk-prepared composites may be seen in Figure 8. At similar w_2, the bulk-

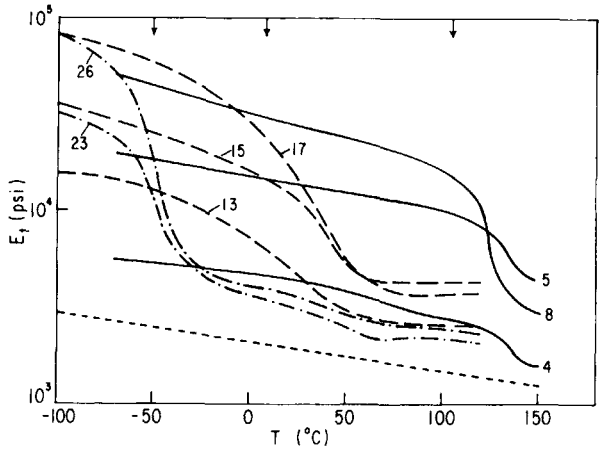

Fig. 7. Torsional modulus–temperature curves for selections of composites for three systems with varied composition, w_2 (Table I). Solid lines represent data for MMA; dashed lines for BA + MMA; broken lines BA. Numbered curves have polymer compositions, w_2, as follows: curve w_2: (4) 0.182; (5) 0.235; (8) 0.470; (13) 0.184; (15) 0.304; (17) 0.523; (23) 0.208; (26) 0.303. Arrows indicate estimated T_g for parent polymer from Fig. 6. Short dashed line is average rate of change of modulus for controls, as in Fig. 6.

prepared composite exhibits more polymer character (Fig. 8) than its emulsion-prepared counterpart. In contrast, at similar ϕ_2 (curve 3) both curves are similar in shape. This again reflects the smaller amount of free space present

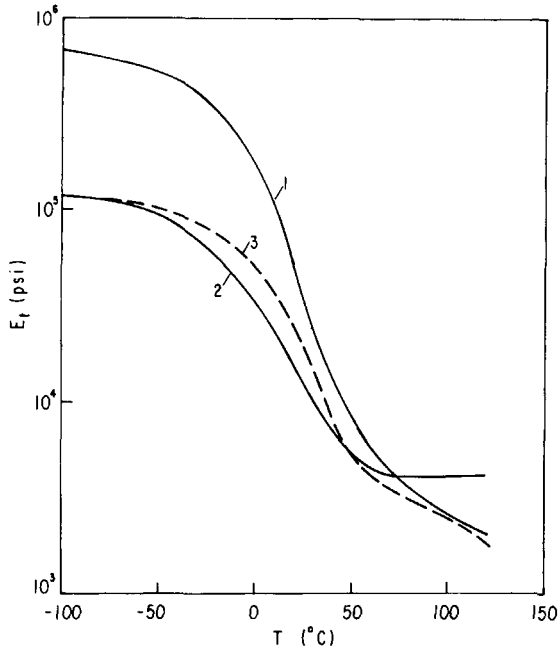

Fig. 8. Torsional modulus–temperature curves for bulk-prepared BA + MMA composite of w_2 = 0.543, curve 1, and emulsion-prepared, methanol-extracted BA + MMA composite of w_2 = 0.579 (ϕ_2 = 0.382), curve 2. Curve 3 is solution prepared BA + MMA composite of ϕ_2 = 0.399 (w_2 = 0.442). Curve shifted down vertically to allow for differences in controls for two systems (Table II).

in bulk-solution systems when compared with emulsion systems at similar w_2 because they have greater density.[1]

In analogy with the data for tensile moduli ratios at 23°C in Figure 3, torsional moduli ratios at 23°C are displayed in Figure 9. The usual experimental scatter and system insensitivity [Fig 9(A)] were again found. Curve-fitted data [solid lines in Figs. 9(B)–9(D)] and Halpin–Tsai [eq. (10)] curves (wide dashed lines) and constants (Table II) are similar to those found for tensile moduli ratios. Consequently, only MMA composites suggest largely parallel mixing; the other system constants in Table II are empirical and the curves are accurate for only a portion of the composite compositions. Reduced moduli ratios at $T_i - 50$°C for all of the torsional moduli data for all systems (MMA, BA + MMA, BA, including all methods of preparation and isolation) fell near a common curve [Fig. 10, (A)]. Although scatter was great, data for the various systems were completely randomized. Curve shape and Halpin–Tsai constants (Table II) resembled those for high-modulus polymers [MMA, Figs. 3(B) and 9(B)], as would be expected. The same collective data, reduced to $T_i + 50$°C [Fig. 10(B)] now resembled curves for BA modification at 23°C [Figs. 3(D) and 9(D)]. Thus, with T_i used as the reference temperature, all three acrylate polymers modified the mechanical properties of leather to a similar extent when prepared with the same polymer volume fractions, regardless of method of preparation or solvent treatment.

Relation between Fiber Aggregation and Polymer Deposition

In the previous discussion, it was observed that fiber aggregation in air-dried, untreated controls resembled polymer deposition in both raising tensile modulus ratios (compared to acetone dried controls) and sample densities. Thus, both treatments reduce free space and introduce transient restraints between fibers to elevate modulus. Similar behavior was found for torsional moduli (Tables I and III). The modulus of the average expanded matrix resulting from acetone treatment of untreated leather [Table I, experiment (1), E_{t1}] was taken as a reference modulus in torsion (E_{t1}) and the average air-dried modulus for controls E_t was obtained from Table III (32,000 psi). With these moduli, the average relative modulus, ln (E_t/E_{t1}), was used together with the fractional increase in density $(\rho_a - \rho_{a1})/(\rho_{a2} - \rho_{a1})$ (0.1024 in this work) to calculate empirical Halpin–Tsai constants (Table II). Modulus ratios for eq. (13) were E_1, 1,944 psi, and E_2, 870,200[28] for pure collagen. The resulting plot [Fig. 11 (A)], defined in a narrow-density range by experimental moduli and densities for the air-dried controls of Table III, suggests that all modulus rise is produced by space loss. Because enhanced frictional restraints resulting from increased fiber contacts are ignored, this cannot be true. Consequently, the characteristic constants A and B, in Table II, are empirical. Use of fractional density increase in the absissa [Fig 11(A)] is justified, however, because $\rho_a = \rho_{a0} + (\rho_{a2} - \rho_{a1})\,\phi_2$, in agreement with eq. (4). Data of Witnauer and Palm[59] on finished leather compressed to various densities gave qualitatively similar increases in modulus but extending over a much wider range of fractional density increase than shown in Fig. 11(A). With these assumptions and qualifications, a modified Halpin–Tsai equation is presented that attributes modulus rise with ϕ_2 for all systems (Figs. 3 and 9) to space loss coupled with enhanced fiber surface interaction, accompanied by

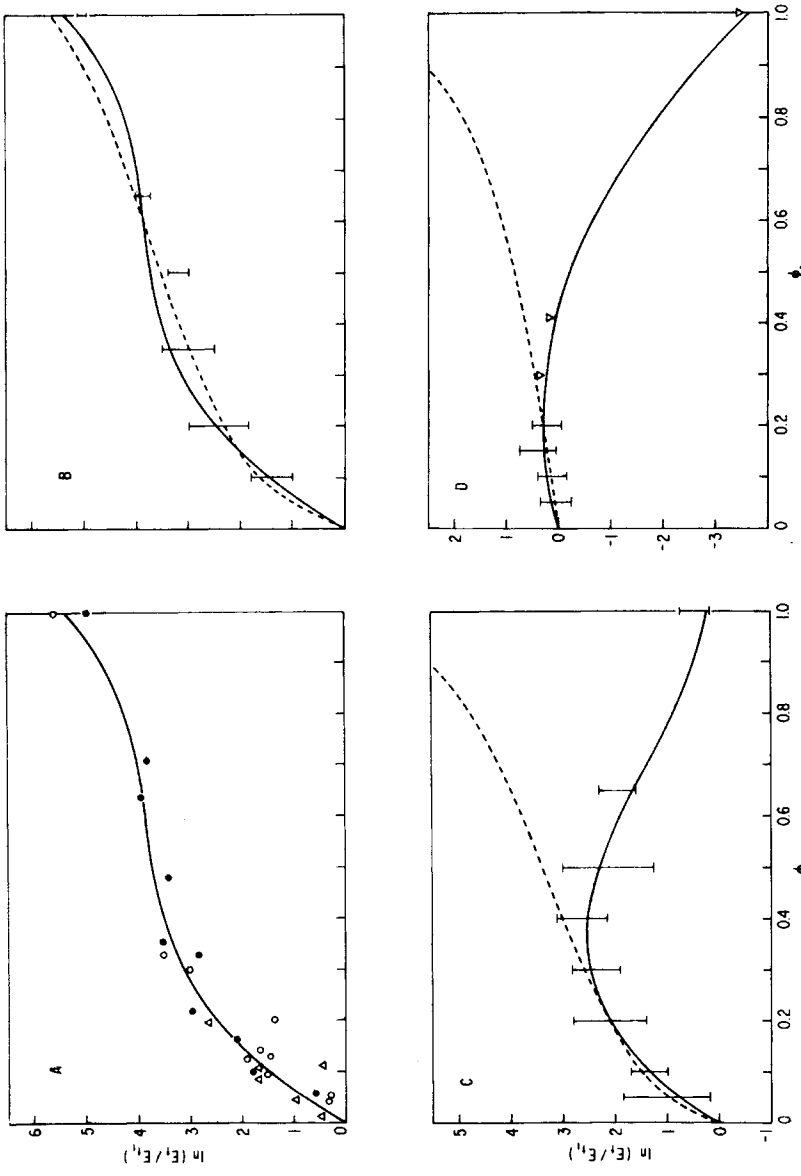

Fig. 9. Log of torsional modulus ratio, $\ln(E_t/E_{t1})$, vs. ϕ_2 for (A) MMA, showing typical experimental scatter exhibited by methanol-extracted experiments (circles), benzene-extracted experiments (triangles), and bulk-solution experiments (solid circles). (B) (MMA), (C) (BA + MMA), and (D) (BA) show curve-fitted [eq. (9)] data (solid line) for same combined systems of (A) and plot of Halpin–Tsai equation [eq. (10)] by use of constants in Table II. Bars express extremes of experimental scatter. Values at highest ϕ_2 are bulk-solution data not listed in Table I.

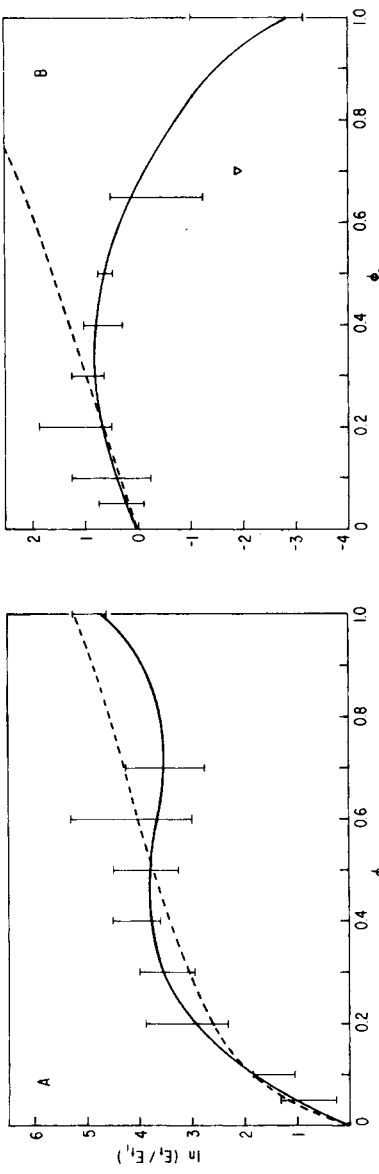

Fig. 10. Log of torsional modulus ratio $\ln(E_l/E_{l1})$ vs. ϕ_2 for insert (A), combined data (methanol-extracted, benzene-extracted, bulk-solution) of all systems (MMA, BA + MMA, BA) at T_i −50°C. (B) Same as (A) but at T_i + 50°C. Bars denote extremes of experimental scatter.

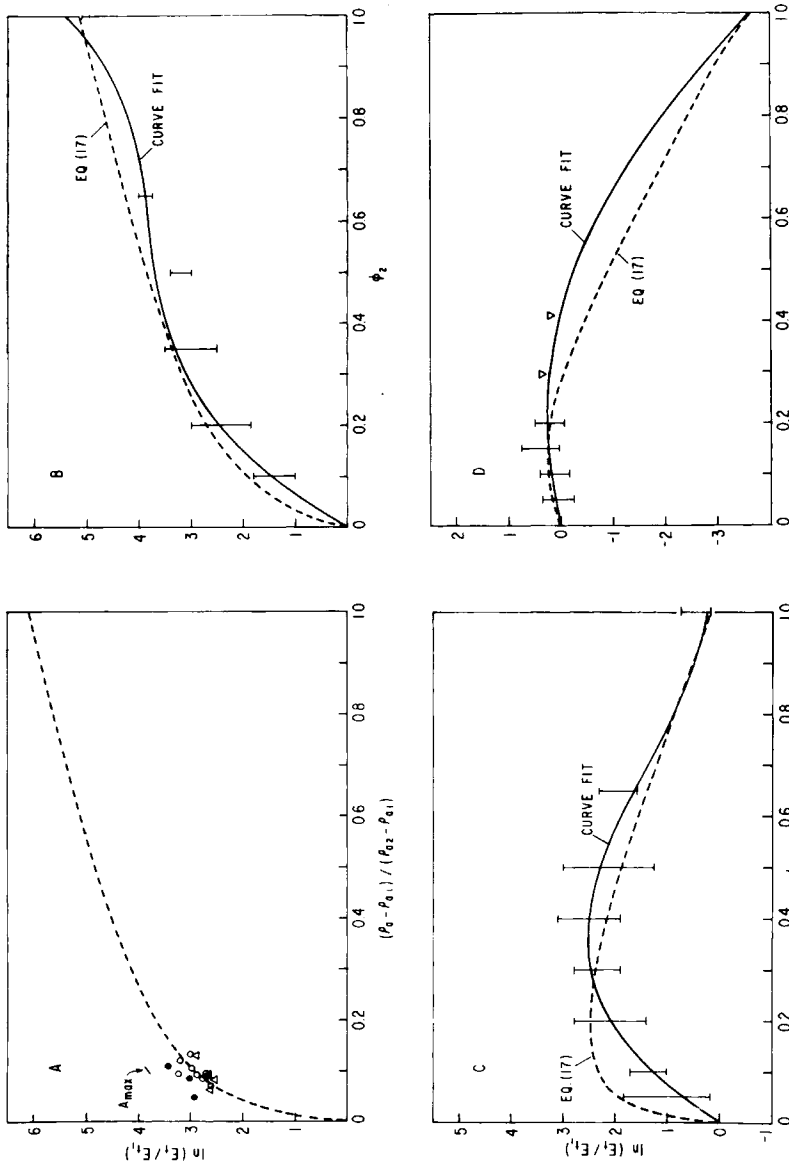

Fig. 11. (A) Log of torsional modulus ratio $\ln(E_i/E_{i1})$ vs. fractional density increase $(\rho_a - \rho_{a1})/(\rho_{a2} - \rho_{a1})$ for all air-dried untreated leather panels (Table III) used with methanol-extracted (circles), benzene-extracted (triangles), and bulk-solution prepared composites (solid circles). Halpin–Tsai equation (10) drawn for averaged values. (B) (MMA), (C) (BA + MMA), (D) (BA), compare curve-fitted data eq. (9), solid lines and eq. (17), dashed lines, by use of constants (Table II) for (A).

a simultaneous modulus change attributed to neat polymer–fiber composite viscoelasticity. The equation is

$$E_t/E_{t1} = [(1 + AB\phi_2)/(1 - A\psi\phi_2)] + C\phi_1 + \phi_2 \ln (E_h/E_c) \quad (17)$$

where $C = K \ln(E_h/E_c)$, K is a constant, and E_c and E_h are the moduli of collagen and the modifying polymer, respectively (Table II). For a reasonable fit of eq. (17) to the data in Figs. 11(B)–11(D) the constants A and B of insert A (Table II) were used. Dependence of $\ln(E_h/E_c)$ for MMA was constant at all ϕ_2, so that $\phi_2 = C' = 1.0$, and K was zero for both MMA and BA + MMA systems [Fig. 11(C)]. For BA [Fig. 11(D)] C was 0.2. These required changes in the adjustable parameters indicate the considerable influence that soft polymers have on reducing stiffness in leather. The curves calculated by use of eq. (17) (wide dashed lines) show fair agreement with the computer-fitted curves [solid lines, eq. (9)] for torsional moduli ratios. They were less successful, however, with tensile moduli data shown as the short dashed lines in Figures 3(B)–3(D) for the same composites. Thus, eq. (17) specifies that the modulus ratios for compressed leathers are initially raised by space depletion necessarily accompanied by segmental fiber interactions that persist, conceptually, until the bulk-collagen state is reached as free space vanishes. For the polymer–leather composites, polymer encasement of fibers and fibrils performs the same function but simultaneously involves the complex relaxation spectrum of neat collagen–leather composites for estimating the relative moduli as composition changes. The terms to the right in eq. (17) express this effect empirically.

Recasting of the function $\phi_2 \ln(E_c/E_h)$ in terms of the Halpin–Tsai constants for BA + MMA composites gave $A = 11.4$ and $B = 0.968$ if ψ is accepted as unity. This suggests a combination of parallel and series mixing contributions for the association between polymer and collagen. It was shown previously (Table II) that mostly parallel mixing of segmentally aligned fibers characterized fiber aggregation. The presence of polymer appears to introduce more isotropic character to polymer–leather composites by intervening between fiber surfaces. Finally, eq. (17) might also predict the mechanical behavior of leather-impregnant mixtures[40–42] and, perhaps, that contributed by fat liquoring agents.[60] The latter act, in low concentration (6–15%), as low-molecular-weight oil dispersants which prevent fiber aggregation in air drying. While these are generally considered to be lubricants, they may actually function as components of composite materials, and thereby, alter collagen surfaces.

SUMMARY AND SIGNIFICANCE

Mechanical properties were obtained on selections from the polymer–leather composite materials prepared in parts I, II, and III. The information presented in this article has already been treated in the synopsis. The significance of these polymer-modified systems in terms of effect on leather properties and as examples of unusual composite materials can be summarized as follows.

These systems, and other similar fibrous compositions, are examples of composite materials composed of three phases, two of which are continuous, one polymeric, and the other fibrous, interspersed by free space that is gradually depleted as polymer content increases. As polymer content was incrementally increased for all three systems in this work, relative stiffness between composite

and untreated control always increased at low-volume fractions of polymer. This was shown to result from the peculiar morphology present, wherein polymer was dispersed in rather coarse domains around individual fibers situated in fiber bundles, leaving the fine structure relatively polymer-free. This type of packing restricted fiber motion and increased composite stiffness. At higher polymer contents, however, the expected more intimate interaction between polymer and fiber, which is more influenced by the glass transition of the modifying polymer, determined the relative stiffness. Figures 3 and 9–11 illustrate these trends. The effect of the modifying polymer on the dynamics of the stress–strain curves resulting from the morphology and polymer content are presented in Figures 1, 2, and 5. It was further observed that any type of filler that reduced matrix free space and encouraged fiber-to-fiber bonding also increased relative stiffness (Figs. 2 and 5). With due allowance for subsequent polymer–fiber interaction, these ideas were incorporated into eq. (17). Finally, the effect of temperature also reflected a tricomponent system composed of polymer, collagen, and free space (Figs. 6 and 7). Both composite systems studied (emulsion deposited and bulk-solution prepared) were rheologically similar when correlated against the volume fraction of polymer used because both contributed similar morphology to the systems.

The authors thank Mr. Americo A. DeMarchis for some of the tensile data and Mrs. Sandra P. Graham for the computer calculations.

References

1. E. F. Jordan, Jr., B. Artymyshyn, A. L. Everett, M. V. Hannigan, and S. H. Feairheller, *J. Appl. Polym. Sci.* (part I), **25,** 2621 (1980).

2. E. F. Jordan, Jr., and S. H. Feairheller, *J. Appl. Polym. Sci.* (part II), **25,** 2755 (1980).

3. E. F. Jordan, Jr., R. J. Carroll, M. V. Hannigan, B. Artymyshyn, and S. H. Feairheller, *J. Appl. Polym. Sci.*, (part III), **26,** 61 (1981).

4. A. H. Korn, S. H. Feairheller, and E. M. Filachione, *J. Am. Leather Chem. Assoc.*, **67,** 111 (1972).

5. A. H. Korn, M. M. Taylor, and S. H. Feairheller, *J. Am. Leather Chem. Assoc.*, **68,** 224 (1973).

6. E. H. Harris, M. M. Taylor, and S. H. Feairheller, *J. Am. Leather Chem. Assoc.*, **69,** 182 (1974).

7. (a) K. Arai, in *Block Graft Polym.*, R. J. Cereso, Ed., John Wiley, New York, 1973 pp. 193–268; (b) pp. 269–310.

8. M. S. Bains, *J. Polym. Sci. Part C,* **37,** 125 (1972).

9. P. L. Nayak, *J. Macromol. Sci. Rev. Macromol. Chem.*, **14,** 193 (1976).

10. M. J. Rollins, A. M. Canizzaro, F. A. Blouin, and J. C. Arthur, Jr., *J. Appl. Polymer Sci.*, **12,** 71 (1968).

11. I. C. Watt, *J. Macromol. Sci. Rev. Macromol. Chem.*, **5,** 175–244 (1970).

12. J. C. Arthur, Jr., in *Adv. Macromol. Chem.*, Vol. 2, W. M. Pasika, Ed., Academic Press, New York, 1970, pp. 1–87.

13. J. C. Arthur, Jr., and R. J. Demint, *Tex. Res. J.*, **30,** 505 (1960).

14. F. A. Blouin, N. J. Morris, and J. C. Arthur, Jr., *Tex. Res. J.*, **38,** 710 (1968).

15. F. A. Blouin, N. J. Morris, and J. C. Arthur, Jr., *Tex. Res. J.*, **36,** 309 (1966).

16. R. Y. M. Huang and W. H. Rapson, *J. Polym. Sci., Part C,* 169 (1963).

17. G. Landrells and C. S. Whewell, *J. Soc. Dyers Colourists,* **71,** 171 (1955).

18. F. A. Blouin, A. M. Cannizzaro, J. C. Arthur, Jr., and M. L. Rollins, *Tex. Res. J.*, **38,** 811 (1968).

19. T. Mares and J. C. Arthur, Jr., *J. Polym. Sci., Part C,* **37,** 349 (1972).

20. I. C. Watt, *J. Macromol. Sci. Chem.*, **4,** 1079 (1970).

21. H. L. Needles, *Tex. Res. J.*, **48,** 506 (1978).

22. D. S. Varma and R. K. Sarkar, *Angew. Makromol. Chem.*, **37,** 177 (1974).

23. N. K. Boardman and L. Lipson, *J. Soc. Dyers Colourists,* **69,** 336 (1953).
24. L. Valentine, *J. Tex. Inst.,* **47,** T1 (1956).
25. M. Feughelman, *Appl. Polym. Symp.,* **18,** 757 (1971).
26. E. Menefee, *Appl. Polym. Symp.,* **18,** 809 (1971).
27. J. R. Kanagy, in *Chemistry and Technology of Leather,* Vol. 4, F. O'Flaherty, W. T. Roddy, and R. M. Lollar, Eds., Reinhold., New York, 1965, pp. 369–416.
28. J. V. Yannas, *J. Macromol. Sci. Rev. Macromol. Chem.,* **7,** 49 (1972).
29. J. R. Kanagy, E. B. Randall, T. J. Carter, R. A. Kinmouth, and C. W. Mann, *J. Am. Leather Chem. Assoc.,* **47,** 726 (1952).
30. R. M. Lollar, *J. Am. Leather Chem. Assoc.,* **54,** 306 (1959).
31. J. R. Kanagy, *J. Am. Leather Chem. Assoc.,* **50,** 112 (1955).
32. H. J. Hodus and R. Stubbings, *J. Am. Leather Chem. Assoc.,* **52,** 414 (1957).
33. E. B. Randall, T. J. Carter, T. J. Kilduff, C. W. Mann, and J. R. Kanagy, *J. Am. Leather Chem. Assoc.,* **47,** 404 (1952).
34. D. H. Russell, *J. Am. Leather Chem. Assoc.,* **52,** 396 (1957).
35. R. E. Whittaker, *J. Soc. Leather Technol. Chem.,* **59,** 172 (1975).
36. A.-L. Nguyen, B. T. Vu, and G. L. Wilkes, *Polym. Prep., Am. Chem. Soc., Div. Poly. Chem.,* **13,** (2), 1003 (1972).
37. L. P. Witnauer and W. E. Palm, *J. Am. Leather Chem. Assoc.,* **56,** 58 (1961).
38. G. O. Conabere and R. H. Hall, *J. Intern. Soc. Leather Chem.,* **30,** 214 (1946).
39. J. Menkert, J. H. Dillon, K. Beurling, and J. G. Fee, *J. Am. Leather Chem. Asssoc.,* **57,** 318 (1962).
40. K. Panduranga, K. T. Joseph, Y. Nayudamma, and M. Santappa, *J. Sci. Ind. Res.,* **33,** 243 (1974).
41. K. N. Zurabjan, *J. Soc. Leather Trades Chem. Assoc.,* **60,** 306 (1968).
42. R. Oehler and T. J. Kilduff, *J. Res. Natl. Bur. Stand.,* **42,** 63 (1949).
43. K. P. Rao, K. T. Joseph, and Y. Nayudamma, *Leather Sci.,* **19,** 27 (1972).
44. K. P. Rao, D. H. Kamat, K. T. Joseph, M. Santappa, and Y. Nayudamma, *Leather Sci.,* **21,** 111 (1974).
45. S. H. Feairheller, E. H. Harris, A. H. Korn, M. M. Taylor, and E. M. Filachione, *Polym. Prepr., Am. Chem. Soc. Div. Polym. Chem.,* **13,** 736 (1972).
46. (a) L. E. Nielsen, in *Mechanical Properties of Polymers and Composites, Parts I and II,* Marcell Dekker, New York, 1974, pp. 379–452; (b) pp. 453–510; (c) pp. 294–299; (d) pp. 257–340; (e) pp. 208–215.
47. J. Williamson, *Brit. Plastics,* **23,** 87 (1950).
48. R. F. Clash, Jr., and R. M. Berg, *Ind. Eng. Chem.,* **34,** 1218 (1942).
49. E. F. Jordan, Jr., B. Artymyshyn, G. R. Riser, and A. N. Wrigley, *J. Appl Polym. Sci.,* **20,** 2737 (1976).
50. M. Mooney, *J. Colloid Sci.,* **6,** 162 (1951).
51. E. H. Kerner, *Proc. Phys. Soc.,* **69,** 808 (1956).
52. Z. Haskin and S. Shtrikman, *J. Mech. Phys. Solids,* **11,** 127 (1963).
53. S. W. Tsai, *U.S. Gov. Rep.* AD 834,851, 1968.
54. J. C. Halpin, *J. Comp. Mater.,* **3,** 732 (1969).
55. M. Takayanagi, H. Harima, and Y. Imata, *Mem. Fac. Eng. Kyushu Univ.,* **23,** 1 (1963).
56. (a) J. A. Manson and J. H. Sperling, in *Polymer Blends and Composites,* Plenum, New York, 1976, pp. 51–334; (b) pp. 62–72.
57. N. Hata and A. V. Tobolsky, *J. Appl. Polym. Sci.,* **12,** 2597 (1968).
58. E. F. Jordan, Jr., B. Artymyshyn, G. R. Riser, and A. N. Wrigley, *J. Appl. Polym. Sci.,* **20,** 2715 (1976).
59. L. P. Witnauer and W. E. Palm, *J. Am. Leather Chem. Assoc.,* **54,** 246 (1963).
60. T. C. Thorstensen, in *Practical Leather Technology,* R. E. Krieger, New York, 1976, pp. 190–207.
61. E. F. Jordan, Jr., G. R. Riser, B. Artymyshyn, J. W. Pensabene, and A. N. Wrigley, *J. Polym. Sci. Part A-2,* **10,** 1659 (1972).

Received June 13, 1980
Accepted July 25, 1980